

Energetics and kinetics of carbonate orientational ordering in vaterite calcium carbonate

JIANWEI WANG* AND UDO BECKER

Department of Earth and Environmental Sciences, University of Michigan, 1100 N. University Avenue, Ann Arbor, Michigan 48109, U.S.A.

ABSTRACT

Vaterite is a less stable anhydrous crystalline calcium carbonate than calcite or aragonite and, thus, a rare mineral in geologic settings. However, vaterite is commonly found in biological environments. The mechanisms of crystal nucleation, transformation, and stabilization of vaterite in host materials remain unresolved. Understanding these issues may lead to answer some fundamental questions such as carbonate formation in geological systems and the intriguing occurrence of vaterite in biological systems. This requires an accurate knowledge of the crystal structure of vaterite and its order-disorder transformation. This study employs molecular-dynamics simulations to understand the thermodynamic stability of vaterite and kinetics of the orientational ordering of the carbonate ions. The results show that the potential energy change from disordered to ordered vaterite is about -11 kJ/mol, which significantly changes the relative stabilities of vaterite with respect to other anhydrous calcium carbonate polymorphs, including amorphous calcium carbonate. The heat capacity of vaterite is estimated to be 102.1 ± 0.4 J/(K·mol), comparable to an experimental result of 91.5 ± 3.8 J/(K·mol). The molecular-dynamics simulations also show similar energies for vaterite with different stacking structures, suggesting possible stacking disordering along the [001] axis. Cyclic high-temperature simulated-annealing molecular-dynamics simulations show that the CO₃ orientational disorder-order transition is thermally activated. The calculated activation energy for the transition is 94 ± 10 kJ/mol with a pre-exponential factor of $\sim 1.6 \times 10^{13}$ s⁻¹. A good linear fit of the logarithmic transition rate to inverse temperature (the Arrhenius plot) indicates that the transition is controlled by a single activation process that is related to a cooperative rotational motion of CO₃ groups in vaterite.

Keywords: Molecular simulation, vaterite, ordering, energetics, kinetics, calcium carbonate

INTRODUCTION

Natural vaterite occurs in biological systems (Ariani et al. 1993; Falini et al. 1998, 2005; Kanakis et al. 2001; Giralt et al. 2001; Sanchez-Moral et al. 2003; Sommerdijk and de With 2008), sediments (Friedman 1997; Giralt et al. 2001), and rocks (Friedman et al. 1993; Grasby 2003), but also in synthetic products such as cement (Stepkowska et al. 2003). Thermodynamically, vaterite is the least stable phase of the three crystalline polymorphs of anhydrous calcium carbonates: calcite, aragonite, and vaterite. Because of its thermodynamic metastability, vaterite is rare in most geologic settings and it transfers to other more stable polymorphs over time under most geologic conditions (Plummer and Busenberg 1982). However, recent studies show that vaterite can easily be grown inorganically under various laboratory conditions (Dalas et al. 1999; Hou and Feng 2005; Seo et al. 2005; Han et al. 2006; Shivkumara et al. 2006; Schlomach et al. 2006; Pouget et al. 2009). Experiments show that rapid mixing of calcium and carbonate salt solutions leads to precipitation of various shapes of fine crystalline vaterite crystals (Han et al. 2006). Vaterite crystals can also be stabilized with additions of biomolecules or organic molecules and are often formed at the surfaces of these molecules in supersaturated solutions by template-induced surface interactions (Ariani et al. 1993; Falini et al. 1998, 2005; Kanakis et al. 2001; Sanchez-Moral et al. 2003; Malkaj and

Dalas 2004; Sommerdijk and de With 2008; Pouget et al. 2009). Vaterite can be formed biogenically as in the case of pearls (Qiao and Feng 2007; Qiao et al. 2008; Soldati et al. 2008), human hearts (Kanakis et al. 2001), and otoliths (Jessop et al. 2008), or non-biogenically as in modern lakes and sediments (Friedman 1997; Giralt et al. 2001; Grasby 2003). It often transforms from an amorphous calcium carbonate (ACC) phase, the metastable precursor of vaterite (Nebel et al. 2008). Therefore, vaterite inherits the disordered character of carbonate ions and the fine particle size of amorphous calcium carbonate. Because of its thermodynamic instability, vaterite formed in these conditions may experience an order-disorder transition (Wang and Becker 2009), or a subsequent transformation to more stable phases such as calcite in rocks and sediments (Plummer and Busenberg 1982; Han et al. 2006).

The crystal structure of vaterite was investigated by single-crystal X-ray diffraction studies (Meyer 1959; Kamhi 1963; Meyer 1969). A hexagonal structure with orientationally disordered CO₃ groups was established. The structure has *P6₃/mmc* symmetry with a basic pseudocell ($Z = 2$) and $a = b = 4.13$ Å and $c = 8.49$ Å (Kamhi 1963). There is only one crystallographic carbonate site in the structure. These early results also suggest possible ordering in the (001) plane and ordering and stacking faults along the [001] direction, both of which are evident from a small number of weak reflections (Kamhi 1963), and numerous diffuse streaks and satellite reflections (Meyer 1969). These observations were attributed to partial superstructure formations.

* E-mail: jwwang@umich.edu

Unfortunately, details of the superstructure (symmetry and coordinates) were not provided due to a lack of high-quality diffraction data and an appropriate structure model. Thus, the structural relation between the ordered and disordered structures is still unresolved. Therefore, it used to be widely accepted in the literature that the orientation of carbonate ions in vaterite is completely random. Continuous efforts have been made to understand the vaterite structure using spectroscopic methods (Sato and Matsuda 1969; Behrens et al. 1995; Anderson 1996; Gabrielli et al. 2000; Wehrmeister et al. 2010). However, issues related to the superstructure, especially the symmetry and number of crystallographic carbon sites in the structure, remain unanswered and a structure model that supports all the spectroscopic results has not established. Recently, a new fully ordered structure model with an orthorhombic symmetry was proposed and this structure was based on X-ray diffraction data and a microtwinning hypothesis (Le Bail et al. 2011). However, five weak superstructure reflections seen in single-crystal X-ray diffraction (Kamhi 1963), and X-ray powder diffraction experiment (Le Bail et al. 2011) are still unexplained. In a previous theoretical study, an ordered superstructure was proposed based on *ab initio* calculations and molecular-dynamics (MD) simulations (Wang and Becker 2009). The superstructure ($Z = 18$) has $P6_322$ symmetry (no. 179) and $a = b = 7.29 \text{ \AA}$, $c = 25.3 \text{ \AA}$, and two unique CO_3 groups (Wang and Becker 2009). This superstructure is consistent with NMR results showing two distinct carbon peaks (Michel et al. 2008). The superstructure is a result of ordering in the **a-b** plane and in the **c** direction and the ordering only involves carbonate ions in the crystal. The lattice vectors **a** and **b** of the superstructure are rotated by 30° with respect to the original basic pseudocell lattice and the lengths are $\sqrt{3}$ times the basic lattice *a* and *b*. Ordering in the **c** direction results in an ordered stacking of three pseudocells by a sixfold rotational symmetry along the **c** axis. Note that this superstructure model (Wang and Becker 2009) was based on the energetics with respect to the disordered structure model (Kamhi 1963) and the ordered orthorhombic structure (Meyer 1959). Although the relation between the superstructure and the supercell proposed by Kamhi (1963) and how to use these structure models to best describe the vaterite structure remain to be explained, the ordered superstructure is energetically more favorable with respect to the disordered structure (Kamhi 1963) and ordered orthorhombic structure (Meyer 1969).

The orientational ordering of CO_3 groups in vaterite has an intrinsic driving force, which is related to electrostatic interactions among CO_3 groups and with the Ca sublattice. In both the ordered and disordered vaterite structures, there are three preferred orientations for each individual CO_3 group in vaterite. This is because each CO_3 is located at the center of a triangular prism formed with the Ca ions and the CO_3 plane is perpendicular to the base faces of the Ca prism. The dominance of the attractive electrostatic interactions between the positively charged Ca^{2+} ions and the negatively charged O centers of CO_3^{2-} groups defines the three orientations, which have a 120° angle between them. Locally within one prism, there is no preference among these three orientations as they are equally energetically favorable. Thus, in a CO_3 orientationally disordered structure, there is no orientational correlation between neighboring CO_3 groups. However, longer-range ordering can reduce the system

potential energy through favorable (or better, less unfavorable) electrostatic interactions by avoiding configurations with the O atoms of neighboring CO_3 groups pointing to each other. However, the details of how the carbonate groups are ordered in vaterite are still in debate in the literature (Wehrmeister et al. 2010; Le Bail et al. 2011).

To understand the disorder to order transition in vaterite, two model systems are considered: the pseudocell structure with one distinct CO_3 (Kamhi 1963) as a model for disordered structure and the superstructure with two distinct CO_3 (Wang and Becker 2009) as a model for the ordered structure. Thermodynamic stability of the ordered and disordered structures and kinetics from the disorder-order transition are investigated using molecular-dynamics simulations. The results are also put in the context of three other anhydrous calcium carbonates. Although the ordered superstructure is more energetically favorable than the disordered structure, the dynamic process of the transition is determined by the kinetics of the order-disorder reaction. Based on previous molecular-dynamics simulations (Wang and Becker 2009), the estimated enthalpy of the transition from disordered vaterite to fully ordered vaterite is -11 kJ/mol or $\sim -4 k_B T$ at ambient condition (how this relates to thermodynamic stabilities of vaterite, aragonite, and calcite will be discussed in the last section). This result implies that, at statistical equilibrium, the majority of vaterite should be at the ordered state. However, it is not clear if a high kinetic barrier prevents this disorder-order transition from occurring at short timescales and/or at ambient temperature. Whether or not such a transition can be observed at an experimental timescale at ambient temperature is in question.

In this paper, the CO_3 order-disordering process in vaterite is investigated using molecular-dynamics simulations. Temperature-annealing simulations are carried out at temperatures higher than ambient to observe a transition within the timescale of the simulations but not too high in order to avoid structural decomposition. Simulations at different temperatures are performed to investigate the temperature effect on the kinetics of the transition. An inherent structure analysis method is used to distinguish the ordered structure from the disordered one, an alternative to energetic analysis. These simulations are designed to systematically investigate the nature of the transition process and the kinetics and energetics of the transition.

METHODS

Molecular models and MD simulations

Three-dimensional periodic boundary conditions are employed in the molecular dynamics using a program package GROMACS (Allen and Tildesley 1987; van der Spoel et al. 2005). Since the 3D periodic boundary conditions require Ewald summation over the long-range electrostatic interactions, which are computationally expensive, the Fast Particle-Mesh Ewald (FPME) summation method is used (Essmann et al. 1995). For van-der-Waals interactions, Lennard-Jones 12-6 potentials are used with a direct-space interaction cutoff distance of 10 \AA . For bonding interactions, harmonic C-O stretching and O-C-O bending, and harmonic improper dihedral interactions for CO_3 are used within the carbonate ion. Non-bonded interactions within the CO_3 group are excluded from the intramolecular interactions because they are part of the bonded and bending interactions. However, non-bonded interactions are included for Ca-Ca, carbonate-carbonate, and Ca-carbonate interactions. The positions of all atoms in the simulation supercell and the supercell parameters are not constrained and therefore free to change. For temperature coupling, the Nose-Hoover thermostat is used, and for pressure coupling, the isotropic Parrinello-Rahman scheme. The

time step for the MD simulations is set to 1 fs, the time constant for temperature coupling to 0.1 ps, and the time constant for pressure coupling to 1.0 ps (van der Spoel et al. 2005).

The forcefield and parameter settings for the MD simulations are similar to those in the previous molecular-dynamics simulations with minor modifications (Wang and Becker 2009) and are tested for the crystallographic cell parameters of calcite and aragonite. A change of the forcefield from the previous simulations (Kalinichev et al. 2001; Wang and Becker 2009) is made for the carbonate intramolecular interaction parameters [harmonic angle O-C-O $c_0 = 520.5$ kJ/mol/(rad)² and harmonic improper dihedral C-O₃ $c_0 = 500.0$ kJ/mol/(rad)²] for better vibrational frequencies and elastic constants. The vibrational frequencies for the three calcium carbonate phases are calculated using the computer program GULP without symmetry constraint (Gale and Rohl 2003). The calculations reproduce major peaks around 1420–1500 and 1040–1080 cm⁻¹ and low frequencies below 500 cm⁻¹ for calcite, aragonite, and vaterite. The results are in qualitative agreement with experimental observations (Wehrmeister et al. 2010). The calculated in-plane bending peaks are scattered from 750 to 900 cm⁻¹, probably resulted from inaccurate improper dihedral forcefield parameters. The calculated elastic constants are overestimated on average by 25% as compared with experimental values (Dandekar and Ruoff 1968). This discrepancy may partially arise from using the simplified forcefield with the Lennard-Jones 12-6 potentials and the single-point charge approximation for oxygen atoms, which may result in higher elastic constants. A more accurate potential for carbonates that was fitted with experimental results including elastic properties is available from literature, where a core-shell model is used for the oxygen atoms (Fisler et al. 2000). However, using the shell model makes MD simulations a lot slower and is not desirable for large-scale long-time simulations as in this study. More recently, a potential for calcium carbonates was developed for simulating nucleation and crystal growth from aqueous solution (Raiteri et al. 2010). Although the forcefield used in the present study produces some errors in elastic constants and vibrational frequencies, for the purpose of the understanding of thermodynamics and kinetics of order-disorder transition in vaterite, the forcefield is expected to be sufficiently accurate to provide a qualitative guide to the nature of the transition. A general introduction of molecular-dynamics simulations is available in Allen and Tildesley (1987) and Frenkel and Smit (2002); the applications on minerals are given in, e.g., de Leeuw and Parker (1998), Cygan (2001), and Piana et al. (2005); and the applications on minerals and their surfaces are reported in, e.g., Wang et al. (2001, 2003, 2006, 2007, 2009), Kirkpatrick et al. (2005a, 2005b), and Kalinichev et al. (2007).

Two simulation supercells with different geometries are used. One is hexagonal and is built from the carbonate-disordered hexagonal structure (Kamhi 1963). The computational supercell has hexagonal dimensions (24.78 × 24.78 × 25.47 Å, 216 CaCO₃ units) and consists of 6 × 6 × 3 unit cells. The experimental structure model provided by Kamhi (1963) has random orientations of carbonate ions with partial occupancies of 1/3 of all C and O atoms. However, for most molecular simulations, partial occupancies are prohibitive. Therefore, our computational supercell with 1080 atoms is constructed by repeating the original unit cell after one of the three possible CO₃-plane orientations is arbitrarily chosen and C and O atoms are assigned an occupancy of unity. Therefore, all carbonate ions in this resulting supercell structure repeat the carbonate orientations and are therefore ordered. Thus, vaterite structures with random carbonate orientations or ordered superstructures have to be generated in a subsequent setup step.

To test the effect of computational supercell geometry on the order-disorder transition of CO₃ orientations and the resulting structure, a starting supercell geometry with an orthorhombic shape is also used (in addition to the hexagonal geometry) for the computational supercell. This orthorhombic supercell is built from the orthorhombic structure (*Pbnm*, $a = 4.13$, $b = 7.15$, and $c = 8.48$ Å) suggested by Meyer (1959). The dimensions of this initial orthorhombic supercell are 24.78 × 21.46 × 25.47 Å, also with 1080 atoms or 216 CaCO₃ units as for the hexagonal case.

Energetics of amorphous calcium carbonate is also simulated for comparison. Recent progress has been made to understand the energetics (Radha et al. 2010) and structure (Nebel et al. 2008; Michel et al. 2008; Goodwin et al. 2010) of ACC. However, the atomic-scale structural details are still unknown. In this study, the structure of ACC is prepared by heating calcium carbonate crystal structures well above their melting temperature and then quenching it to 0 K in NPT-ensemble MD simulations. Two ACC models are used and they are based on two separate MD simulations with two different starting configurations. Such models are used to estimate their relative energetic stability with respect to other polymorphs. Note that such models may not be accurate representatives of the ACC structure, but they are expected to be adequate for a qualitative estimate of the energetics.

MD simulated annealing

Simulated-annealing MD simulations are carried out to study the effect of temperature on the order-disorder transition in vaterite. The method is implemented by simply varying the reference temperature in an NPT ensemble (constant temperature and pressure) during the simulation. The difference between the simulated annealing MD and a standard MD is that the system temperature in the former is controlled by a set of reference temperatures and may be cycled one or more times in between a temperature minimum and maximum (van der Spoel et al. 2005). The annealing protocol is specified as a series of corresponding times and reference temperatures. Two kinds of simulated annealing MD are performed. In the first kind, the temperature is linearly increased from 0 K to a maximum temperature of 1600 K in 15 ns. In the second kind, the temperature is linearly increased from 0 K to a given maximum temperature and then back to 0 K in a cyclic fashion. Four cycles of the reference temperatures are applied in sequence in the simulations: 0–300–0 K, 0–500–0 K, 0–1000–0 K, and 0–1500–0 K, for 1.25, 1.25, 1.5, and 2.5 ns for each cycle, respectively. The reference temperature is changed by about 0.5–1.2 K/ps or every 1000 time steps (the time step = 1 fs, 1 ps = 1000 fs). Since the temperature increment is small, ~1 K/ps, no equilibration time is applied between or during the cycles. The time constant for temperature coupling and pressure coupling are the same as those in the standard MD simulations.

Inherent structure

To determine the time for the transition from the disordered to the ordered vaterite to take place, standard constant-temperature and constant-pressure ensemble MD simulations (NPT) are carried out at 750, 800, 850, 900, 950, 1000, 1200, and 1400 K. The simulation times vary from 1 to 500 ns, depending on the simulation temperature. At each temperature, a frame is saved in every 50 ps. Each such frame of the trajectory is subsequently optimized by energy minimization. This optimized structure is the inherent structure of the corresponding structure at the high temperature (Stillinger and Weber 1983). By analyzing the inherited structures for symmetry, which is used to better distinguish the ordered structures from the disordered ones, the transition time is determined. Since there is an ~11 kJ/mol energy difference between the disordered and the ordered structures, an alternative method to determine the transition time is to analyze the potential energy. The two methods are expected to give the same results. The symmetry information provides more accurate structural information and can be readily obtained from the inherent structure where atoms are close to their equilibrium positions. However, this approach can be difficult for structures at high temperature where atoms are away from their equilibrium positions. The order-disorder transition times at different temperatures are analyzed using the Arrhenius relation.

RESULTS AND DISCUSSION

Variation of potential energy as a function of temperature

The potential energy change of vaterite with increasing temperature is revealed using simulated annealing MD simulations. By continuously changing the reference temperature of the system from 0 to 1600 K (in increments of ~0.1 K/ps) in the MD simulation, the potential energy as a function of the simulation time and the statistical temperature is recorded. As temperature increases, there are statistically meaningful changes of the slope of the potential energy with the simulation time (Fig. 1a) and with the system temperature (Fig. 1b). These changes are highlighted by the dashed- (Fig. 1a) and dot-dashed (Fig. 1b) lines. An abrupt or steep change in energy with temperature indicates a crystal-structure change, which can be analyzed by examining the MD trajectory.

At the beginning of the MD simulation, the vaterite structure is ordered, which is constructed with the carbonate orientation arbitrarily ordered as described in the Methods section. This ordering persists for ~3 ns until the temperature reaches ~300 K after which the carbonate-ion orientation becomes disordered. During this re-orientation of carbonate ions, the potential energy drops by 22 kJ/mol. This energy change is consistent with the previous molecular-dynamics simulations (Wang and Becker 2009). This

result indicates that the initially arbitrarily ordered structure is unstable with respect to the disordered structure. In this disordered structure, the CO_3 groups are randomly distributed over three possible orientations, which is consistent with the disordered vaterite structure model (Kamhi 1963). For a separate and similar MD simulation with an orthorhombic (instead of hexagonal) computational supercell where the CO_3 groups are also initially ordered (the orthorhombic Meyer structure), a similar structural disordering is observed at a similar temperature (~ 320 K), accompanying an energy drop of 19 kJ/mol. This result suggests that the structure with disordered CO_3 groups is energetically more favorable than the arbitrarily ordered structure based on the basic hexagonal structure (Kamhi 1963) and the ordered orthorhombic structure (Meyer 1959).

From 3 to 14 ns in the MD simulation (Fig. 1a), while the system temperature continuously increases from 300 to 1600 K (Fig. 1b), the slope of potential energy as a function of temperature changes, which is caused by a continuous change in the structure without a definite phase change. It needs to be mentioned that at any point in the MD simulation, the system may not reach the

equilibrium with the given temperature because of short simulation time (short in terms of actual macroscopic growth processes but relatively long in the framework of MD simulations). The orientations of the CO_3 groups become gradually more and more ordered with increasing simulation time and temperature. Such structural ordering with temperature indicates a thermally activated process that drives the change of the CO_3 orientations and causes the orientational ordering of the carbonate ions.

The orientational ordering of the CO_3 groups and the associated potential energy change as a function of temperature are better mimicked by cyclic simulated-annealing MD simulations at different annealing temperatures. Figure 2a shows the potential energy of the system with the simulation time from a sequence of such cyclic annealing simulations. For each annealing cycle, the system temperature starts from 0 K, and then reaches the annealing temperature and decreases to 0 K. Each succeeding cycle of the annealing process reduces the potential energy of the system from that of the previous cycle. The potential energy is reduced by 22, 2, 5, and 4 kJ/mol for the systems annealed at the annealing temperatures of 300, 500, 1000, and 1500 K,

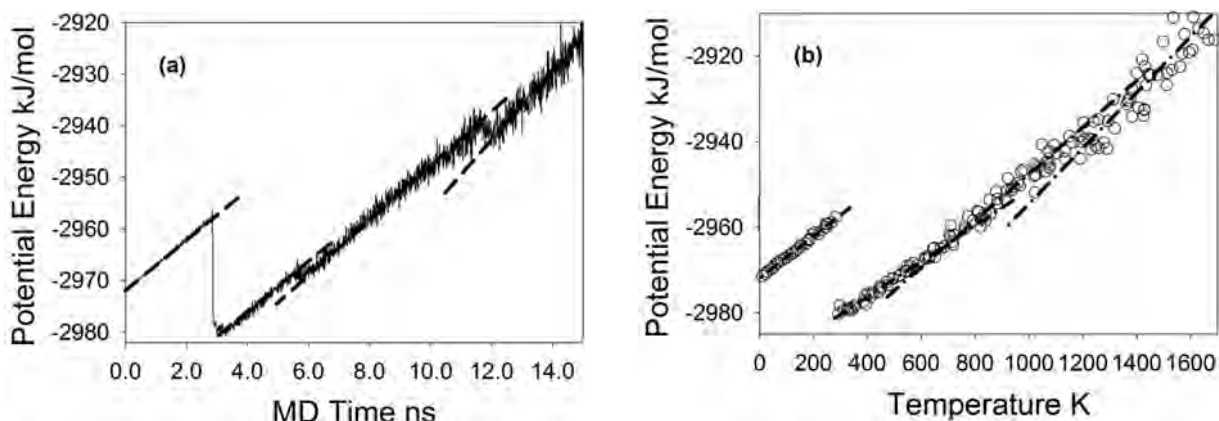


FIGURE 1. Potential energy of vaterite as a function of molecular-dynamics simulations time (a) and temperature (b) in a single simulated annealing MD simulation. The dashed lines are guides to the eye. The data line in a is the potential energy from the MD trajectory recorded at 10 ps intervals. The open circles are the average values of system potential energies and temperature recorded at 100 ps intervals.

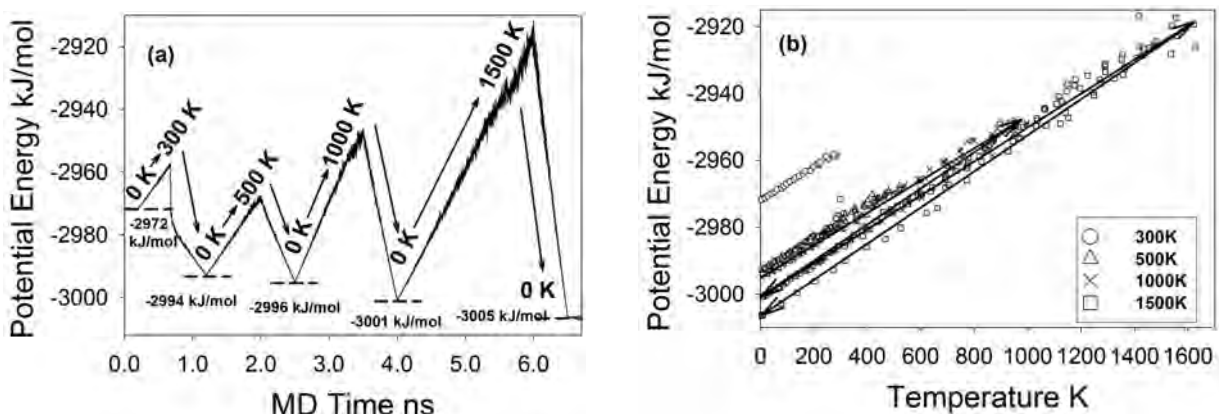


FIGURE 2. Potential energy of vaterite as a function of molecular-dynamics simulations time (a) and temperature (b) in four cyclic simulated annealing MD simulations. The solid arrowed lines in b trace the potential energy vs. temperature for the temperature cycles of 0–1000–0 K and 0–1500–0 K.

respectively. Figure 2b shows the potential energy change with the system temperature. For each cycle, the energy change with temperature traces a different energy-temperature path with a different slope, resulting in a different potential energy at the end of each annealing cycle at 0 K. The total change of potential energy before and after the annealing cycles is -33 kJ/mol, and the energy change from the disordered structure to the ordered one is -11 kJ/mol. Since the structure at 300 K is not strictly disordered, the estimated disorder-to-order transition energy provides an upper limit and the real transition energy may be more negative. Because the potential energy reduction of the structure at the end of each cycle is affected by the simulation temperature and simulation time, the orientational disordering and ordering transition are expected to be kinetically controlled and activated by thermal energy. Note that the energy difference calculated is the potential energy difference without corrections for zero-point energies and entropic contributions.

The slope changes of the potential energy as a function of temperature during the different cycles of the simulations indicate changes in the heat capacity at different order-disorder states of vaterite. These slope changes are highlighted by the solid arrowed lines in Figure 2b, which trace the potential energy as a function of temperature for the last two annealing cycles: 0–1000–0 K and 0–1500–0 K. For both cycles, the slope during temperature increase (i.e., from 0 K to the annealing temperature) is different from that during temperature decrease (i.e., from the annealing temperature to 0 K). The classical heat capacity at constant pressure can be obtained from equation $C_p = (\partial H / \partial T)_p$, where enthalpy $H = U + PV$, U is the total energy, P is the system pressure, and V is the system volume (Forsblom and Grimvall 2005). By a linear fit of enthalpy as a function of temperature, the heat capacity at constant pressure can be calculated. For the disordered vaterite, the calculated value is 102.1 ± 0.4 J/(K·mol) in a temperature range from 300 to 350 K. For the ordered vaterite, the value is 112.0 ± 0.9 J/(K·mol) in the same temperature range (Table 1). The standard errors are a result of from the linear fit. The ordered vaterite has a higher heat capacity. The experimentally measured constant pressure heat capacity is 91.5 ± 3.8 J/(K·mol) at 353 K (Wolf et al. 2000). Considering that there might be substantial disordering in experimental samples of vaterite (Wang and Becker 2009), the calculated heat capacity of the disordered vaterite is comparable with the observation (Wolf et al. 2000). In classical molecular-dynamics simulations, reliabilities of the simulations depend on accuracies of the interatomic potentials used in the simulations, which often need to be appropriately calibrated with known physical properties of the systems. Given that the forcefield parameters are not calibrated with properties related to the energetics of vaterite and its temperature dependence, such an agreement on the heat capacity between the theoretical calculation and the observation may be fortuitous.

Carbonate ion orientational ordering in vaterite

The orientational ordering of CO_3 groups in vaterite results in a superstructure that is transformed from the disordered structure by increasing temperature in the molecular-dynamics simulations. The ordering is thermally activated and accompanied by a decrease in potential energy. Snapshots from the cyclic simulated-annealing MD simulations at different annealing temperatures are used to qualitatively illustrate the ordering process. For the annealing simulation at 300 K, there is a very limited ordering of CO_3 orientations (Fig. 3a). Most of the three CO_3 groups in each column along [001] are distributed only in one or two directions. The ordering of the structure is identified by comparing it with the superstructure with a hexagonal $P6_322$ symmetry. As the annealing temperature increases from 300 to 500 K, more and more columns of the CO_3 groups become ordered (Fig. 3b). For the structure at annealing temperature of 1500 K (Fig. 3c), all the columns of the CO_3 groups are ordered and the structure has the $P6_522$ symmetry. To better describe the ordering, an order parameter is defined as $O_{\text{CO}_3} = \sum o_i / 3N$, where o_i is the number of orientations of CO_3 in column i , and N is the total number of columns in the system. If O_{CO_3} is 1.0, the system is ordered. For the initial arbitrarily ordered structure, O_{CO_3} is $1/3$. For the random orientation of CO_3 , O_{CO_3} is ~ 0.7 . As the annealing temperature increases from 300, 500, 1000, to 1500 K, the order parameter increases from 0.6, 0.7, 0.8 to 1.0, respectively, suggesting increasing ordering as the annealing temperature increases. Note that Figure 3 and the order parameter only provide approximate information about the ordering along the [001] direction. The ordered superstructure needs a quantitative symmetry analysis. The unit cells are highlighted in Figure 3c for the pseudo-cell structure and the hexagonal superstructure.

To test if the three-dimensional periodic boundary conditions and the hexagonal computational cell employed in the MD simulations have any effect on CO_3 orientational ordering and the resulting structure and symmetry in the ordered vaterite, additional simulated annealing MD simulations are performed using a different computational supercell with an orthorhombic geometry and the same number of atoms. The energetics of the orientational disorder-to-order transition with this model (figures are not shown) are similar to the ones presented in Figures 1 and 2. The structural changes at different annealing temperatures with this orthorhombic computational supercell are also similar to those shown in Figure 3. However, the smallest repeating unit of the final annealed ordered structure has a monoclinic symmetry of $C2/c$ (space group no. 15) and $a = 12.62$ Å, $b = 7.29$ Å, $c = 9.37$ Å, and $\beta = 115.9^\circ$. Figure 3c highlights the monoclinic repeating unit in the (001) plane, which is closely related to the hexagonal unit cell. Along the [001] direction, however, the orientational

TABLE 1. Thermodynamic properties of vaterite and thermodynamic/kinetic parameters of its disorder-order transition

Properties		MD calculation	Experiment
Heat capacity [C_p , J/(K·mol)]	Disordered	102.1 ± 0.4 (300–500 K)	91.5 ± 3.8 (353 K)*
	Ordered	112.0 ± 0.9 (300–500 K)	
Enthalpy of transition (kJ/mol)		10.6 ± 0.5	
Transition kinetics	Activation barrier (kJ/mol)	93.9 ± 9.6	
	Pre-exponential factor	1.6×10^{13}	

* Experimental results are based on calorimetric and potentiometric measurements (Wolf et al. 2000).

ordering is different. Figure 4a shows the structural ordering of the hexagonal superstructure with the unit cell highlighted, and the c dimension, which is three times the one of the disordered pseudo-cell. Figure 4b shows the structural ordering based on the orthorhombic geometry along the same direction. The repeating unit length in the $[001]$ direction of the latter is equal to that of the pseudo-cell. Apparently, the simulation conditions (e.g., supercell geometry) affect the structural ordering in the $[001]$ direction but not in the (001) plane. This result suggests that ordering in the (001) plane is more robust and may have

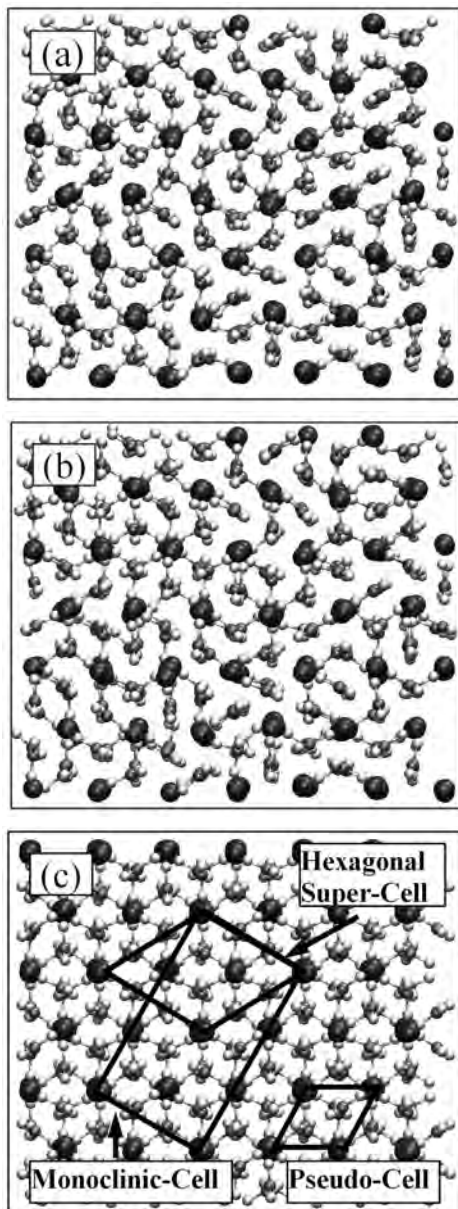


FIGURE 3. Final structures of vaterite annealed at different temperatures: (a) 300 K cycle, (b) 500 K, and (c) 1500 K. Large black balls are Ca ions, small gray balls are C atoms, and white balls are O atoms. In c, unit cells in the (001) plane are highlighted for the basic pseudo-hexagonal cell, monoclinic supercell, and hexagonal supercell.

a larger energetic driving force than that in $[001]$ direction. A careful evaluation of the two structures (Figs. 4a and 4b) indicates different stacking sequences, implying a high possibility for disordered stacking in vaterite, which was hypothesized in an early single X-ray diffraction study (Kamhi 1963). While the monoclinic structure ($C2/c$) has not been suggested for vaterite, a group of closely related high-temperature phases of rare earth orthoborates were found with the same monoclinic structure (Lin et al. 2004).

To estimate the relative stability of the monoclinic unit-cell superstructure with respect to the hexagonal superstructure, an ab initio structural optimization of the monoclinic cell similar to the previous study (Wang and Becker 2009) is carried out. The total energy for the monoclinic cell is energetically slightly more stable with respect to the hexagonal superstructure cell by ~ 10 kJ/mol, which is of the same order of disorder-to-order transition energy. The small energy difference indicates possibilities of different ways of structural ordering along $[001]$, which could result in stacking disordering. This probably is the

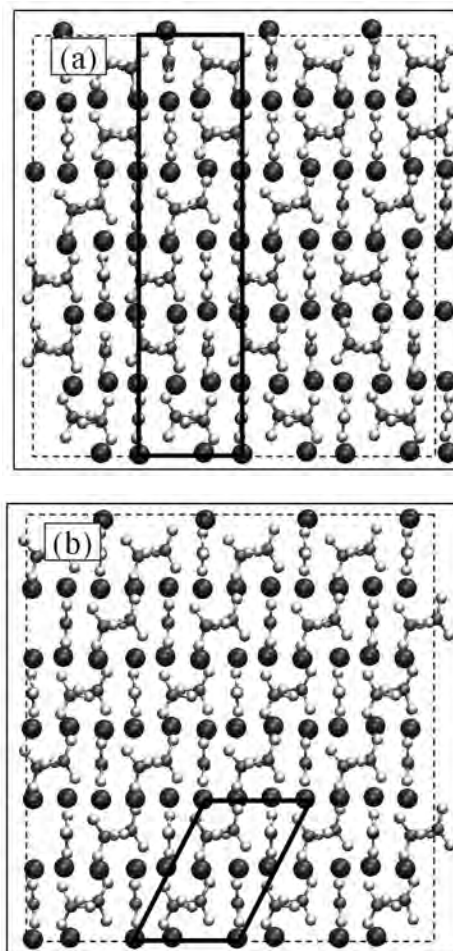


FIGURE 4. Final ordered vaterite after annealing viewed perpendicular to $[001]$: (a) using the hexagonal computational cell (the structure shown is after conversion to an orthorhombic cell, for better comparison with b), and (b) using an orthorhombic computational cell. The unit cells are highlighted.

reason that there are extensive stacking faults in the samples previously suggested by single X-ray diffraction experiments (Meyer 1959, 1969; Kamhi 1963).

Kinetics of the thermally activated order-disorder transition

The kinetics of the thermally activated disorder-order transition is studied using standard-NPT-ensemble MD simulations. The disorder-order transition time t_{tr} is defined as the time for a disordered vaterite structure to transfer to the ordered structure at a given temperature during the MD simulation. The t_{tr} is determined by inspecting and analyzing the symmetry of the inherent structure of each frame of the recorded MD trajectory. To speed up the transition, the system is heated up to high temperatures of up to 1400 K. The chosen simulation temperatures are high enough for the transition to occur within half a microsecond (i.e., half a billion simulation time steps), which can be reasonably achieved in to an MD simulation with available computational resources. The results are shown in Table 2. The transition rate is defined as $1/t_{tr}$. An Arrhenius plot of the CO₃ orientational disorder-to-order transition is shown in Figure 5. A linear fit results in an activation energy of 93.9 ± 9.6 kJ/mol and a pre-exponential factor of $\sim 1.6 \times 10^{13}$ s⁻¹ (Table 1). The standard error is derived from the linear fit of $\ln(1/t_{tr})$ as a function of $1/T$. The correlation coefficient R of the fit is 0.996, indicating a single thermally activated disorder-order transition. The calculated activation energy for the order-disorder transition is less than half of the activation energies for the vaterite-to-calcite phase transition of 250 ± 10 kJ/mol (Baitalow et al. 1998) and vaterite decomposition of 227 kJ/mol (Maciejewski et al. 1994). The latter two processes require a much higher energy to be activated because they involve significant structural rearrangement and complete structural destruction. The pre-exponential factor for the disorder-order transition is close to the rotational frequency of CO₃ in vaterite, which is around ~ 300 cm⁻¹ (or $\sim 1 \times 10^{13}$ Hz) (Behrens et al. 1995). This result indicates that orientational ordering may be related to the rotational motion of CO₃ groups. It is intuitive that the full structural ordering is associated with the orientational ordering of the individual CO₃ groups, but it is not clear how they are related. The activation energy of a single CO₃ rotation can be estimated by gradually rotating a single carbonate ion about the *c* axis in a series of molecular dynamic calculations at low temperatures at which the re-orientational movement of the rest CO₃ groups is not active. The calculated activation energy is 195 kJ/mol at 100 K, 187 kJ/mol at 200 K, and 186 kJ/mol at 300 K, which are close to the activation energy of

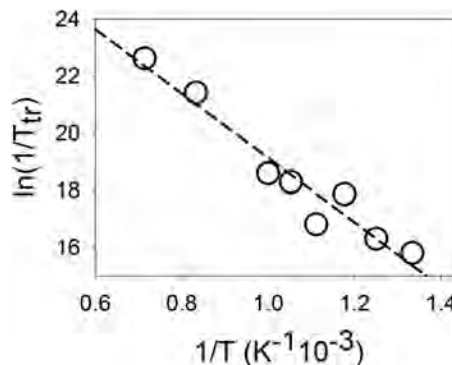


FIGURE 5. Arrhenius plot of CO₃ orientational disorder-to-order transition. The transition time t_{tr} is estimated by inspecting the inherent structures of each frame of the trajectory recorded at 50 ps intervals of standard NPT-ensemble MD simulations at a given temperature. $1/t_{tr}$ is evaluated as the reaction rate.

vaterite decomposition. However, these values for individual carbonate ions are about two times higher than the result for the whole system (i.e., ~ 94 kJ/mol), suggesting that the orientational ordering in the structure is not isolated reorientation of each individual CO₃ group but a cooperative movement among CO₃ groups. As a result of the carbonate reorientation, there is a volume contraction of 0.47% from the disordered structure to the ordered structure (Wang and Becker 2009).

Based on the values of the calculated activation energy and pre-exponential factor, the disorder-to-order transition is fast and should be complete within an hour at ambient temperature. However, caution should be taken for directly comparing the simulation result with an experimental observation. Experimentally synthesized vaterite samples often have impurities such as organic molecules as interfacial stabilizing agents (Falini et al. 2005; Sommerdijk and de With 2008; Pouget et al. 2009) and their role on disorder-order transition is unknown. In addition, inaccuracy in the empirical potentials used to mimic the energetics of the carbonate system in the MD simulations may cause some errors in the absolute values of the kinetics. Nevertheless, the MD results provide a theoretical basis for understanding order-disorder phenomena in vaterite. Direct evidence of the orientational ordering of CO₃ groups and the superstructure may be observable on vaterite samples using single-crystal X-ray diffraction or nanoscale local structural analysis techniques such as high-resolution transmission electron microscopy. These experiments would also provide additional information about the nature of the ordered structure in vaterite such as size of ordered regions and stacking sequences. However, the theoretical results are expected to provide valuable information for predictions and guidance for designing new experiments. For instance, X-ray powder diffraction patterns for vaterite at different degrees of ordering were calculated from structures based on the P6₃22 model in a previous study (Wang and Becker 2009). Those results show that the diffraction peaks in the range of $2\theta \approx 38\text{--}44^\circ$ identified as the superstructure peaks in a recent X-ray diffraction study (Le Bail et al. 2011) were predicted by the calculations (Wang and Becker 2009).

TABLE 2. Orientational disorder-order transition of carbonate ions in vaterite at different temperatures

Simulation temperature (K)	Transition time (t_{tr} , ns)	$1/T (\times 10^{-3})$	$\ln(1/t_{tr})$
1400	0.15	0.7143	22.6204
1200	0.50	0.8333	21.4164
1000	8.50	1.0000	18.5832
950	11.50	1.0526	18.2809
900	50.00	1.1111	16.8112
850	17.50	1.1765	17.8611
800	83.00	1.2500	16.3044
750	137.00	1.3333	15.8033

TABLE 3. Enthalpy differences of aragonite and vaterite (ordered and disordered) with respect to calcite (unit: kJ/mol)

Phase	MD (a)	MD (b)	DFT numerical basis (c)	DFT plane-wave (d)	DFT plane-wave (e)	DFT (PAW-GGA) (f)	DFT linear-scaling (g)	Experiments
amorphous	+26.6(a') +28.5(a')							+15.0 (h), +14.3 (i), +22.7 (j), +17.2 (k), +12.3 (l)
vaterite (dis)	+20.7			+16.39	+17.54	+19.80		+6.2 (m) +3.4 (n)
vaterite (ord)	+9.7		+5.00	+2.95	+5.72	+5.80	–	
aragonite	–3.0	–4.8 ~ +12.67	+8.6	+0.996	+12.69	+12.19	–4.9 ~ +9.3	+1.2 (m) –0.4 (n)
calcite (reference)	0.0	0.0	0.00	0.00	0.00	0.00	0.0	0.0

Notes: (a) Molecular-dynamics simulations (Wang and Becker 2009). (a') Molecular-dynamics simulations (this study). The structures for ACC are produced by heating calcium carbonate crystal structure well above its melting temperature and then quenched to 0 K. Two models are based on separated simulations. (b) Calculated enthalpy differences for literature forcefields for CaCO₃ (Raiteri et al. 2010). (c–f) This study. (c) DFT with numerical basis sets using program DMol³. (d) DFT with plane-wave basis sets using CASTEP and norm-conserving pseudopotentials. (e) DFT with plane-wave basis sets using CASTEP and ultrasoft pseudopotentials. (f) DFT with plane wave basis sets using VASP and GGA-PAW methods. (g) DFT with norm-conserving pseudopotentials and a flexible, numerical linear combination of atomic orbitals basis set using SIESTA (Raiteri et al. 2010). (h) Experiment based on thermoanalysis of ACC crystallization (Wolf and Gunther 2001). (i) Average value of the calorimetric measurements of anhydrous ACC (Radha et al. 2010). (j) Average value of the calorimetric measurements of more disordered hydrous ACC (Radha et al. 2010). (k) Average value of the calorimetric measurements of less disordered hydrous ACC (Radha et al. 2010). (l) Experiment based on thermoanalysis of ACC crystallization (Koga et al. 1998). (m) Experiments based on the dissociation reactions measurements (Plummer and Busenberg 1982). (n) Experiments based on calorimetric and potentiometric measurements (Wolf et al. 1996, 2000).

Energetics of vaterite ordering and thermodynamic stability of anhydrous calcium carbonate polymorphs

Because of the typically small crystal sizes and rare occurrence of vaterite in geological settings, vaterite has not drawn much attention from mineralogy and materials science communities. Recent experiments (Kanakakis et al. 2001; Malkaj and Dalas 2004; Han et al. 2006; Pouget et al. 2009) suggest that vaterite as well as its stability and formation in both biogenic and abiogenic settings are complex and many aspects of the related processes are yet to be explored. The present molecular-dynamics simulations of the order-disorder transition further the understanding of the phase stability of vaterite. Thus, it is important to discuss the energetics and kinetics of the order-disorder transition of vaterite in the context of other calcium carbonate polymorphs.

The degree of disordering in vaterite affects its relative stabilities with respect to the other polymorphs: amorphous calcium carbonates (ACC), aragonite, and calcite. Table 3 lists the enthalpy differences of various anhydrous calcium carbonate polymorphs with respect to calcite from both experiments and theoretical calculations available from the literature and results from this study. These data are also plotted in Figure 6. The enthalpy difference between aragonite and calcite varies widely and even changes signs among different theoretical calculations. Experiments give small values on the enthalpy difference: 1.2 kJ/mol (Plummer and Busenberg 1982) and –0.4 kJ/mol (Wolf et al. 1996, 2000). For the ordered vaterite, the calculated enthalpy is 3–10 kJ/mol higher than calcite, in comparison with experimental values of 6.2 kJ/mol (Plummer and Busenberg 1982) and 3.4 kJ/mol (Wolf et al. 1996, 2000), which are between the minimum and maximum calculated energy difference. The experimental values are based on as-made samples and the degree of disordering was not evaluated. It is expected, however, that those samples have at least some degree of ordering up to being completely ordered. Theoretical calculations suggest that the enthalpy of the disordered vaterite is 11–14 kJ/mol above the ordered vaterite. For disordered vaterite, four theoretical calculations show that the enthalpy is 16–21 kJ/mol higher than calcite as shown in Table 3. There is no experimental value for the disordered vaterite.

For ACC, the experimental enthalpy is 12.3–22.7 kJ/mol higher than calcite, which is comparable to the calculated values of the disordered vaterite. The calculated enthalpy for ACC is 26.2 and 28.5 kJ/mol higher than calcite from two MD calculations based on two different structure models for ACC. The calculated values for ACC are higher than the experimental values probably because of the accuracy of the structural models used for ACC. However, the comparison between ACC and disordered vaterite is only qualitative. For the experiments of ACC, the value varies widely between different experiments and samples with different degrees of disorder, which was not quantified and it would be difficult to do so. Thus, it is difficult to make

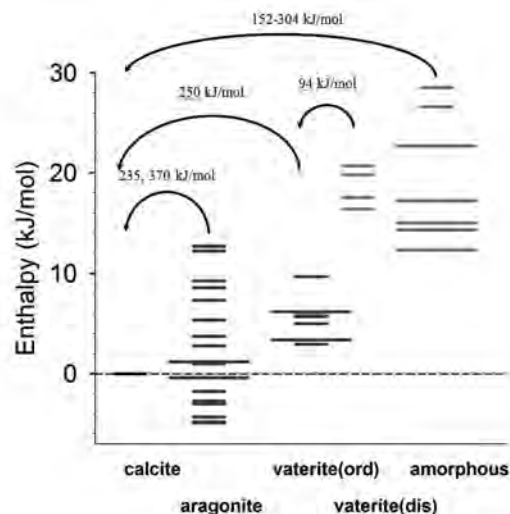


FIGURE 6. Enthalpy differences of different calcium carbonate polymorphs with respect to calcite and activation energies for phase transitions. The thin dashed line is the enthalpy of calcite as reference. Long, thick lines are experimental values. Short, thick lines are values from theoretical calculations. The values of the enthalpies are listed in Table 3. The curved lines with arrows show possible phase transitions documented in the literature and the values above the curves are the activation energy of the transition.

quantitative comparison if structural parameters, such as degree of disorder, of ACC are not identified and determined. Nonetheless, it is expected that the enthalpy of disordered vaterite should not be much lower than the one of ACC, given that enthalpy of disordered vaterite is 16–21 kJ/mol higher than calcite. These data (Table 3, Fig. 6), regardless of the discrepancies between different experiments and theoretical calculations, suggest that the degree of disordering in vaterite has a large effect on the relative stability of vaterite with respect to ACC, aragonite, and calcite. The effect is enhanced by the fact that there are only small energy differences among the three crystalline polymorphs (e.g., ordered vaterite, aragonite, and calcite) and between ACC and disordered vaterite. In addition, the size effect on free energies of calcium carbonate precipitates could complicate the relative stabilities of the different polymorphs.

The kinetics of the phase transitions also plays an important role to control the formation and growth of different calcium carbonate polymorphs. The activation energy for the order-disorder transitions of vaterite is ~94 kJ/mol, which is much smaller than ~250 kJ/mol for the vaterite to calcite transition (Peric et al. 1996; Baitalov et al. 1998; Wolf and Gunther 2001), 235 kJ/mol (Peric et al. 1996) or 370 kJ/mol (Wolf and Gunther 2001) for the aragonite to calcite transition based on the two experiments, and 152–304 kJ/mol for ACC to calcite transition (Koga et al. 1998). These data suggest a faster ordering transition in vaterite than its transition to calcite. In solution, however, indirect transformations through dissolution-recrystallization processes may have much lower activation energies. For instance, for the vaterite to calcite transition in solution, the activation energy is only ~55 kJ/mol (Kralj et al. 1997). Other factors, such as surfaces of organic molecules, may also affect the kinetics of the transitions, especially of these less stable polymorphs of calcium carbonates (i.e., ACC and vaterite). Currently, a full description of phase stabilities and kinetics of the transitions of various calcium carbonate polymorphs is far from being completed. It is expected that such knowledge is essential to the understanding of the nucleation, growth, and transformation of calcium carbonates in various conditions relevant to calcium carbonate formations in natural systems.

ACKNOWLEDGMENTS

We acknowledge the support by the National Science Foundation NIRT grant (EAR-0403732). This research was supported in part by the National Science Foundation through the Extreme Science and Engineering Digital Environment (XSEDE) resources provided by NCSA and NICS under grant TG-DMR080047N and TG-DMR100034.

REFERENCES CITED

- Accelrys (1999) Forcefield-based simulations—Cerius² user manual. Accelrys: Accelrys Software Inc., San Diego.
- Allen, M.P. and Tildesley, D.J. (1987) *Computer Simulation of Liquids*. Clarendon Press, Oxford.
- Anderson, A. (1996) Group theoretical analysis of the ν_1 (CO_3^{2-}) vibration in crystalline calcium carbonate. *Spectroscopy Letters*, 29, 819–825.
- Ariani, A.P., Wittmann, K.J., and Franco, E. (1993) A comparative study of static bodies in mysid crustaceans: Evolutionary implications of crystallographic characteristics. *Biological Bulletin*, 185, 393–404.
- Baitalov, F., Wolf, G., and Schmidt, H.G. (1998) Thermochemical investigations of calcium carbonate phase transitions—I. Thermal activated vaterite-calcite transition. *Journal of Thermal Analysis and Calorimetry*, 52, 5–16.
- Behrens, G., Kuhn, T.L., Ubig, R., and Heuer, H.A. (1995) Raman spectra of vateritic calcium carbonate. *Spectroscopy Letters*, 28, 983–995.
- Cygan, R.T. (2001) Molecular modeling in mineralogy and geochemistry. In R.T. Cygan and J.D. Kubicki, Eds., *Molecular Modeling Theory and Applications in the Geosciences*, 42, p. 1–35. Reviews in Mineralogy and Geochemistry, Mineralogical Society of America, Chantilly, Virginia.
- Dalas, E., Klepetsanis, P., and Koutsoukos, P.G. (1999) The overgrowth of calcium carbonate on poly(vinyl chloride-co-vinyl acetate-co-maleic acid). *Langmuir*, 15, 8322–8327.
- Dandekar, D.P. and Ruoff, A.L. (1968) Temperature dependence of elastic constants of calcite between 160 degrees and 300 degrees K. *Journal of Applied Physics*, 39, 6004–6009.
- de Leeuw, N.H. and Parker, S.C. (1998) Surface structure and morphology of calcium carbonate polymorphs calcite, aragonite, and vaterite: An atomistic approach. *Journal of Physical Chemistry B*, 102, 2914–2922.
- Essmann, U., Perera, L., Berkowitz, M.L., Darden, T., Lee, H., and Pedersen, L.G. (1995) A Smooth Particle Mesh Ewald Method. *Journal of Chemical Physics*, 103, 8577–8593.
- Falini, G., Fermani, S., Gazzano, M., and Ripamonti, A. (1998) Oriented crystallization of vaterite in collagenous matrices. *Chemistry—A European Journal*, 4, 1048–1052.
- Falini, G., Fermani, S., Vanzo, S., Miletic, M., and Zaffino, G. (2005) Influence on the formation of aragonite or vaterite by otolith macromolecules. *European Journal of Inorganic Chemistry*, 2005, 162–167.
- Fisler, D.K., Gale, J.D., and Cygan, R.T. (2000) A shell model for the simulation of rhombohedral carbonate minerals and their point defects. *American Mineralogist*, 85, 217–224.
- Forsblom, M. and Grimvall, G. (2005) Heat capacity of liquid Al: Molecular dynamics simulations. *Physical Review B*, 72, 132204.
- Frenkel, D. and Smit, B. (2002) *Understanding Molecular Simulation from algorithms to applications*. Academic Press, New York.
- Friedman, G.M. (1997) A re-examination of reported lacustrine vaterite formation in Holkham Lake, Norfolk, UK—Opinion. *Journal of Sedimentary Research*, 67, 616.
- Friedman, G.M., Schultz, D.J., Guo, B.Y., and Sanders, J.E. (1993) Vaterite (an uncommon polymorph of CaCO_3)—occurrences in boreholes demonstrate unexpected longevity. *Journal of Sedimentary Petrology*, 63, 663–664.
- Gabrielli, C., Jaouhari, R., Joiret, S., and Maurin, G. (2000) In situ Raman spectroscopy applied to electrochemical scaling. Determination of the structure of vaterite. *Journal of Raman Spectroscopy*, 31, 497–501.
- Gale, J.D. and Rohl, A.L. (2003) The General Utility Lattice Program (GULP). *Molecular Simulation*, 29, 291–341.
- Giralt, S., Julia, R., and Klerkx, J. (2001) Microbial biscuits of vaterite in Lake Issyk-Kul (Republic of Kyrgyzstan). *Journal of Sedimentary Research*, 71, 430–435.
- Goodwin, A.L., Michel, F.M., Phillips, B.L., Keen, D.A., Dove, M.T., and Reeder, R.J. (2010) Nanoporous structure and medium-range order in synthetic amorphous calcium carbonate. *Chemistry of Materials*, 22, 3197–3205.
- Grasby, S.E. (2003) Naturally precipitating vaterite ($\mu\text{-CaCO}_3$) spheres: Unusual carbonates formed in an extreme environment. *Geochimica et Cosmochimica Acta*, 67, 1659–1666.
- Han, Y.S., Hadiko, G., Fuji, M., and Takahashi, M. (2006) Crystallization and transformation of vaterite at controlled pH. *Journal of Crystal Growth*, 289, 269–274.
- Hou, W.T. and Feng, Q.L. (2005) A simple method to control the polymorphs of calcium carbonate in CO_2 -diffusion precipitation. *Journal of Crystal Growth*, 282, 214–219.
- Jessop, B.M., Shiao, J.C., Iizuka, Y., and Tzeng, W.N. (2008) Prevalence and intensity of occurrence of vaterite inclusions in aragonite otoliths of American eels *Anguilla rostrata*. *Aquatic Biology*, 2, 171–178.
- Kalinichev, A.G., Wang, J., and Kirkpatrick, R.J. (2001) Structure of carbonate and bicarbonate aqueous solutions: Molecular simulation of ionic hydration and ion pairing. Eleventh Annual V.M. Goldschmidt Conference abstract number, 3293.
- Kalinichev, A.G., Wang, J.W., and Kirkpatrick, R.J. (2007) Molecular dynamics modeling of the structure, dynamics and energetics of mineral-water interfaces: Application to cement materials. *Cement and Concrete Research*, 37, 337–347.
- Kamhi, S. (1963) On the structure of vaterite CaCO_3 . *Acta Crystallographica*, 16, 770–772.
- Kanakis, J., Malkaj, P., Petroheilos, J., and Dalas, E. (2001) The crystallization of calcium carbonate on porcine and human cardiac valves and the antimicrobial effect of sodium alginate. *Journal of Crystal Growth*, 223, 557–564.
- Kirkpatrick, R.J., Kalinichev, A.G., and Wang, J.W. (2005a) Molecular dynamics modelling of hydrated mineral interlayers and surfaces: structure and dynamics. *Mineralogical Magazine*, 69, 289–308.
- Kirkpatrick, R.J., Kalinichev, A.G., Wang, J.W., Hou, X.Q., and Amonette, J.E. (2005b) Molecular modeling of the vibrational spectra of interlayer and surface species of layered double hydroxides. In J.T. Kloprogge, Ed., *Application of Vibrational Spectroscopy to Clay Minerals and Layered Double Hydroxides*, 13, p. 239–285. The Clay Mineral Society, Aurora, Colorado.
- Koga, N., Nakagoe, Y.Z., and Tanaka, H. (1998) Crystallization of amorphous calcium carbonate. *Thermochimica Acta*, 318, 239–244.
- Kralj, D., Brecevic, L., and Kontrec, J. (1997) Vaterite growth and dissolution in

- aqueous solution III. Kinetics of transformation. *Journal of Crystal Growth*, 177, 248–257.
- Le Bail, A., Ouhenia, S., and Chateigner, D. (2011) Microtwinning hypothesis for a more ordered vaterite model. *Powder Diffraction*, 27, 16–21.
- Lin, J.H., Sheptyakov, D., Wang, Y.X., and Allenspach, P. (2004) Structures and phase transition of vaterite-type rare earth orthoborates: A neutron diffraction study. *Chemistry of Materials*, 16, 2418–2424.
- Maciejewski, M., Oswald, H.R., and Reller, A. (1994) Thermal transformations of vaterite and calcite. *Thermochimica Acta*, 234, 315–328.
- Malkaj, P. and Dalas, E. (2004) Calcium carbonate crystallization in the presence of aspartic acid. *Crystal Growth and Design*, 4, 721–723.
- Meyer, H.J. (1959) *Versammlungsberichte. Angewandte Chemie*, 71, 673–681.
- (1969) Struktur und fehlordnung des vaterits. *Zeitschrift für Kristallographie*, 128, 183–212.
- Michel, F.M., MacDonald, J., Feng, J., Phillips, B.L., Ehm, L., Tarabrella, C., Parise, J.B., and Reeder, R.J. (2008) Structural characteristics of synthetic amorphous calcium carbonate. *Chemistry of Materials*, 20, 4720–4728.
- Nebel, H., Neumann, M., Mayer, C., and Epple, M. (2008) On the structure of amorphous calcium carbonate—A detailed study by solid-state NMR spectroscopy. *Inorganic Chemistry*, 47, 7874–7879.
- Peric, J., Vucak, M., Krstulovic, R., Brecevic, L., and Kralj, D. (1996) Phase transformation of calcium carbonate polymorphs. *Thermochimica Acta*, 277, 175–186.
- Piana, S., Reyhani, M., and Gale, J.D. (2005) Simulating micrometre-scale crystal growth from solution. *Nature*, 438, 70–73.
- Plummer, L.N. and Busenberg, E. (1982) The solubilities of calcite, aragonite and vaterite in CO₂-H₂O solutions between 0 and 90 °C, and an evaluation of the aqueous model for the system CaCO₃-CO₂-H₂O. *Geochimica et Cosmochimica Acta*, 46, 1011–1040.
- Pouget, E.M., Bomans, P.H.H., Goos, J., Frederik, P.M., de With, G., and Sommerdijk, N. (2009) The initial stages of template-controlled CaCO₃ formation revealed by cryo-TEM. *Science*, 323, 1455–1458.
- Qiao, L. and Feng, Q.L. (2007) Study on twin stacking faults in vaterite tablets of freshwater lacklustre pearls. *Journal of Crystal Growth*, 304, 253–256.
- Qiao, L., Feng, Q.L., and Liu, Y. (2008) A novel bio-vaterite in freshwater pearls with high thermal stability and low dissolubility. *Materials Letters*, 62, 1793–1796.
- Radha, A.V., Forbes, T.Z., Killian, C.E., Gilbert, P., and Navrotsky, A. (2010) Transformation and crystallization energetics of synthetic and biogenic amorphous calcium carbonate. *Proceedings of the National Academy of Sciences*, 107, 16438–16443.
- Raiteri, P., Gale, J.D., Quigley, D., and Rodger, P.M. (2010) Derivation of an accurate force-field for simulating the growth of calcium carbonate from aqueous solution: A new model for the calcite-water interface. *Journal of Physical Chemistry C*, 114, 5997–6010.
- Sanchez-Moral, S., Canaveras, J.C., Laiz, L., Saiz-Jimenez, C., Bedoya, J., and Luque, L. (2003) Biomediated precipitation of calcium carbonate metastable phases in hypogean environments: A short review. *Geomicrobiology Journal*, 20, 491–500.
- Sato, M. and Matsuda, S. (1969) Structure of vaterite and infrared spectra. *Zeitschrift für Kristallographie*, 129, 405–410.
- Schlomach, J., Quarch, K., and Kind, M. (2006) Investigation of precipitation of calcium carbonate at high supersaturations. *Chemical Engineering & Technology*, 29, 215–220.
- Seo, K.S., Han, C., Wee, J.H., Park, J.K., and Ahn, J.W. (2005) Synthesis of calcium carbonate in a pure ethanol and aqueous ethanol solution as the solvent. *Journal of Crystal Growth*, 276, 680–687.
- Shivkumara, C., Singh, P., Gupta, A., and Hegde, M.S. (2006) Synthesis of vaterite CaCO₃ by direct precipitation using glycine and L-alanine as directing agents. *Materials Research Bulletin*, 41, 1455–1460.
- Soldati, A.L., Jacob, D.F., Wehrmeister, J., and Hofmeister, W. (2008) Structural characterization and chemical composition of aragonite and vaterite in freshwater cultured pearls. *Mineralogical Magazine*, 72, 579–592.
- Sommerdijk, N. and de With, G. (2008) Biomimetic CaCO₃ mineralization using designer molecules and interfaces. *Chemical Reviews*, 108, 4499–4550.
- Stepkowska, E.T., Perez-Rodriguez, J.L., Sayagues, M.J., and Martinez-Blanes, J.M. (2003) Calcite, vaterite and aragonite forming on cement hydration from liquid and gaseous phase. *Journal of Thermal Analysis and Calorimetry*, 73, 247–269.
- Stillinger, F.H. and Weber, T.A. (1983) Inherent structure in water. *The Journal of Physical Chemistry*, 87, 2833–2840.
- van der Spoel, D., Lindahl, E., Hess, B., van Buuren, A.R., Apol, E., Meulenhoff, P.J., Tieleman, D.P., Sijbers, A.L.T.M., Feenstra, K.A., van Drunen, R., and Berendsen, H.J.C. (2005) Gromacs user manual version 3.3, www.gromacs.org. University of Groningen.
- Wang, J. and Becker, U. (2009) Structure and carbonate orientation of vaterite (CaCO₃). *American Mineralogist*, 94, 280–286.
- Wang, J.W., Kalinichev, A.G., Kirkpatrick, R.J., and Hou, X.Q. (2001) Molecular modeling of the structure and energetics of hydrotalcite hydration. *Chemistry of Materials*, 13, 145–150.
- Wang, J., Kalinichev, A.G., Amonette, J.E., and Kirkpatrick, R.J. (2003) Interlayer structure and dynamics of Cl-hydrotalcite: Far infrared spectroscopy and molecular dynamics modeling. *American Mineralogist*, 88, 398–409.
- Wang, J., Kalinichev, A.G., and Kirkpatrick, R.J. (2006) Effects of substrate structure and composition on the structure, dynamics, and energetics of water at mineral surfaces: A molecular dynamics modeling study. *Geochimica et Cosmochimica Acta*, 70, 562–582.
- Wang, J., Rustad, J.R., and Casey, W.H. (2007) Calculation of water-exchange rates on aqueous polynuclear clusters and at oxide-water interfaces. *Inorganic Chemistry*, 46, 2962–2964.
- Wang, J., Kalinichev, A.G., and Kirkpatrick, R.J. (2009) Asymmetric hydrogen bonding and orientational ordering of water at hydrophobic and hydrophilic surfaces: A comparison of water/vapor, water/talc, and water/mica interfaces. *Journal of Physical Chemistry C*, 113, 11077–11085.
- Wehrmeister, U., Soldati, A.L., Jacob, D.E., Hager, T., and Hofmeister, W. (2010) Raman spectroscopy of synthetic, geological and biological vaterite: a Raman spectroscopic study. *Journal of Raman Spectroscopy*, 41, 193–201.
- Wolf, G. and Gunther, C. (2001) Thermophysical investigations of the polymorphous phases of calcium carbonate. *Journal of Thermal Analysis and Calorimetry*, 65, 687–698.
- Wolf, G., Lerchner, J., Schmidt, H., Gamsjager, H., Konigsberger, E., and Schmidt, P. (1996) Thermodynamics of CaCO₃ phase transitions. *Journal of Thermal Analysis*, 46, 353–359.
- Wolf, G., Konigsberger, E., Schmidt, H.G., Konigsberger, L.C., and Gamsjager, H. (2000) Thermodynamic aspects of the vaterite-calcite phase transition. *Journal of Thermal Analysis and Calorimetry*, 60, 463–472.

MANUSCRIPT RECEIVED SEPTEMBER 1, 2011

MANUSCRIPT ACCEPTED APRIL 24, 2012

MANUSCRIPT HANDLED BY BIJAYA KARKI